

Study of the Ionospheric Effects of Selected Cases of Solar Flares over Abidjan

Jean Baptiste Ackah, Olivier Kouadio Obrou and Sylvain Malan Ahoua

Laboratoire de Physique de l'Atmosphère, Université Félix Houphouët Boigny Abidjan, 22 B.P. 582 Abidjan 22, Côte-d'Ivoire

Abstract: The present study investigates the changes in TEC (total electron content) and ionospheric scintillation index (S_4) inferred from the GNSS data recorded at the SCINDA station of Abidjan (Latitude = 5.34° N, Longitude = 3.90° W) during and after a solar flare. In the course of 2014, a year of high solar activity, three (3) cases of extreme (X1.66) and moderate (M6.23 and M2.13) solar flares recorded in the months of September and December effects on the ionosphere have been studied using the X ray fluxes, the magnetic parameters (V_x , B_z , Dst), the ionospheric scintillation index S_4 and TEC and its ROT (time rate of change). The ROT exhibits a prominent peak between ten (10) and twelve (12) minutes after the occurrence of the maximum peak of the time rate of change of the X-ray flux emitted during the flare. The ROT maximum value occurs simultaneously with an enhancement of the S_4 index. Deferred perturbations of the solar flare on the TEC in the SCINDA station of Abidjan occur within 42 to 54 hours after an M-class solar flare and within 46 to 58 hours following an X-Class solar flare. The magnetic storms resulted from these flares show an increment of 20% on VTEC observed when compared to the average VTEC ($\langle VTEC_{quiet} \rangle$) computed from the most five (5) quietest days of the selected months.

Key words: TEC, ionospheric scintillation, solar flare, X-ray.

1. Introduction

A solar flare can be defined as the sudden and explosive release of energy ($\sim 10^{19}$ - 10^{25} J) from a localized active region of the Sun usually near a complex group of sunspot, mainly in the form of electromagnetic radiation across the entire spectrum [1]. When the radiation impinges on the earth's ionosphere, several ionospheric disturbances are produced by increasing the ionization level. The solar flares occurring near the central meridian produce much stronger impact than those occurring at the solar limb [2]. The amount of fluxes during the flares varies considerably. But still there is no method by which we can take care of the variation of fluxes in flares while investigating the ionospheric influences of solar flares.

In Western and Asian regions, several studies [3-7] have been conducted in the past to investigate the ionospheric influences of solar flares. It has been

found that the value of f_{min} (frequency of minimum reflection of D layer) increases during the flares and in the case of large flares there can be a complete radio blackout [8]. These disruptions or fadeouts occur as result of increased absorption of radio waves due to increased flare time ionization in the D region. The huge X-ray flux emitted during flares is responsible for causing these fadeouts as the major portion of the flux is able to penetrate to the D region. Lui et al. [9] have examined solar flare signatures on the ionospheric GPS TEC (total electron content). They find that the maximum value of the TEC increase solely depends on the flare class while the maximum value of the time rate of change of TEC increase is related to not only the flare class but also the time rate of change in flare radiations. Early investigators demonstrated that the most likely regions for observing scintillations were near the magnetic equator [10].

The present paper is focused on TEC, S_4 index and the time rate of change of TEC during an X-class and

Corresponding author: Jean Baptiste ACKAH, engineer in meteorology, research field: space science.

M-class solar flares variations at a station located under the influence of the equatorial electrojet where few research of this kind have been conducted so far.

2. Data Used and Method of Analysis

2.1 Data Sets

This work uses the X-ray flux associated with the solar flare recorded by the satellite GOES-15. The data are stored in a free access data based at the following address <ftp.swpc.noaa.gov>. The solar magnetic parameters such as the x component of the solar wind speed V_x and the z component of the magnetic field B_z are recorded by a sensor on board the satellite ACE (advanced composition explorer). The data of one (1) minute resolution as well as the Dst index (SYM/H) have been freely downloaded at http://omniweb.gsfc.nasa.gov/form/omni_min.html.

The raw data of the scintillation index S_4 and the TEC are from the SCINDA station of Abidjan (Latitude = 5.34° N, Longitude = 3.90° W). The TEC, expressed in TECU (1 TECU is equivalent to 10^{12} electrons per cm^2) is defined as the integral of the electron density along the signal path from a satellite to a receiver while S_4 (dimension less) is the ratio of the signal intensity standard deviation by the signal intensity mean. S_4 and TEC are expressed respectively as follow:

$$S_4 = \frac{\sqrt{(I^2) - \langle I \rangle^2}}{I} \quad (1)$$

$$TEC = \int_R^S N_e ds \quad (2)$$

where I is the signal amplitude and N_e the ionospheric electron density. Due to the hardware timing biases and cycle slips on the estimation of the TEC along a line of sight, the TEC value needs to be calibrated by subtracting satellite and receiver inter-frequency biases. The calibration technique used for this study is the one proposed by Carrano et al. [11]. The S_4 and TEC recorded at a rate of one minute are averaged regardless the PRN of the satellite transmitting the signals to the receiver. The S_4 and TEC values are

selected for which the elevation angle of the satellite signal is higher than 30° , in order to avoid the effect of multipath [12]. The Q days used in the study have been selected based on the criteria of the Kyoto World Data Center for Geomagnetism (<http://q/wdc.kugi.kyoto-u.ac.jp/qddays/>). The TEC of the five (5) quietest days of September and December 2014 were selected to compute the reference value of TEC to study the magnetic storm that resulted from the solar flare.

2.2 Method of Analysis

The observed TEC used in this study referred as $VTEC_{observed}$ is obtained using the maximum value of TEC computed from the satellite signal. At every minute, $VTEC_{observed}$ is defined as follows:

$$VTEC_{observed}(t) = \text{Max}(VTEC_{(t)}) \quad (3)$$

Following Shimeis et al. [6] the mean averaged of TEC over the five (5) most magnetic quietest days is defined as follows

$$\langle VTEC_{quiet}(t) \rangle = \frac{1}{5} \sum_{i=1}^5 VTEC_{(t,i)} \quad (4)$$

$\langle VTEC_{quiet}(t) \rangle$ expressed the average over the five i^{th} days at a single time t . The time rate of change of X-ray (rXray) flux emitted during the solar flare and that of the TEC (ROT) are estimated respectively by Eq. (5) and Eq. (6):

$$rXray_{(t)} = \frac{Xray_{(t)} - Xray_{(t-\Delta t)}}{\Delta t} \quad (5)$$

$$ROT_{(t)} = \frac{TEC_{(t)} - TEC_{(t-\Delta t)}}{\Delta t} \quad (6)$$

3. Results

3.1 Study of the Solar Flare

3.1.1 Case 1

Fig. 1 shows the variation of the X-ray from 10 to 12 September 2014 as recorded by the satellite GOES15.

The blue and red curves represent the X-ray flux recorded respectively in the spectra rages $0.5-4.0 \text{ \AA}$ and $(1.0-8.0 \text{ \AA})$. A flare of class X1.66 was observed

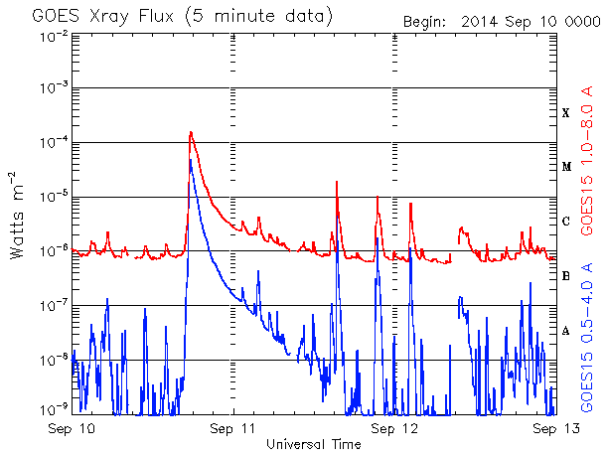


Fig. 1 X-ray flux variation recorded from September 10th to 13th, 2014 (<ftp://ftp.swpc.noaa.gov/pub/warehouse>).

during that time period, precisely around 1600 UT on 10 September. The X-ray flux associated to that flare shows a peak at 17:55 UT (17:35 LT) that decrease to a normal level at around 20:00 UT. Fig. 2 is a plot of the variation of the time rate of change of X-ray (top), the time rate of change of TEC (middle) and the ionospheric scintillation index (bottom) on September, 10th 2014 from 17:00 UT to 18:00 UT. During this time interval that surround the occurrence of a X1.66 class flare, the rate of change of the X-ray flux increase from a lower value of 1.0×10^{-6} W/m²/min to a maximum value 1.66×10^{-5} W/m²/min at 17:43 UT (17:23 LT) (Fig. 2a). The X-ray flux and the ROT exhibits an abrupt and pronounced rise of about 31.16 TECU/min at 17:44 UT (17:24LT) (Fig. 2b), twelve (12) minutes after the occurrence of the rXRay peak. It is practically at the same time that the S₄ index reaches a maximum value estimated to 0.84, characterizing a high ionospheric scintillation (Fig. 2c) due to rapid fluctuation of the TEC as indicated above.

3.1.2 Case 2

Fig. 3 shows the variation of the solar X-ray flux intensity associated with a M6.16 class solar flare that in time ranging from December 3 to 5, 2014.

During this time period, the X-ray flux increases from 10^{-5} W/m² on December 4th to a maximum value of about 6.16×10^{-5} W/m² at 18:25 UT (18:05 LT). Fig. 4 describes the variation of rXRay, ROT and S₄ index

on December 4th from 18:00 UT to 19:00 UT. We observe a peak of rXRay with a maximum value of 2.00×10^{-5} W/m²/min around 18:24 UT (Fig. 4a). The variation of the ROT on December 4th in the time ranging from 18:00 UT (17:40 LT) to 19:00 UT (18:40 LT) shows marked increase of 35.16 TECU/min at 18:34 UT (Fig. 4b). This peak is observed about ten (10) minutes after that of the rXRay. The scintillation index exhibits a higher value (0.65) at the same time indicating an intense ionospheric scintillation phenomenon (Fig. 4c).

3.2 Study of the Magnetic Storm 12-13 September 2014

The magnetic storm resulted from the solar flare is

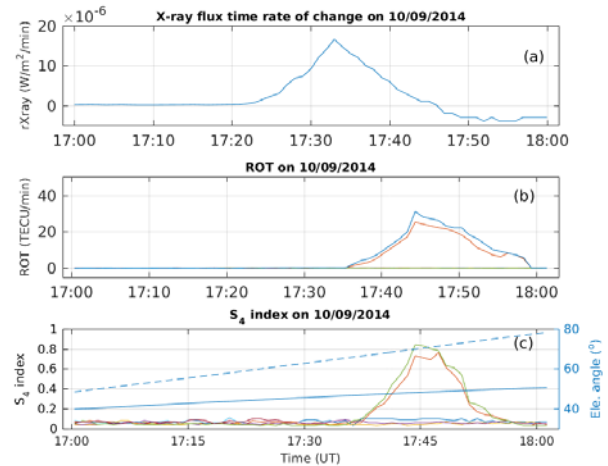
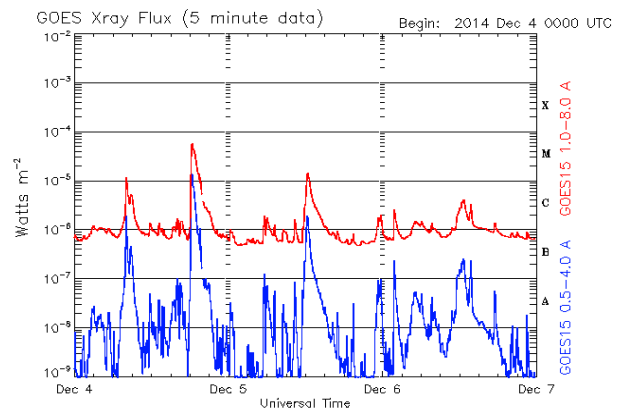


Fig. 2 Variation of rXRay (a), ROT (b) and S₄ index (c) on September 10th 2014 from 17:00 to 18:00 UT.



Updated 2014 Dec 6 23:55:12 UTC NOAA/SWPC Boulder, CO, USA
Fig. 3 X-ray flux variation recorded from December 3rd to 5th, 2014 (<ftp://ftp.swpc.noaa.gov/pub/warehouse>).

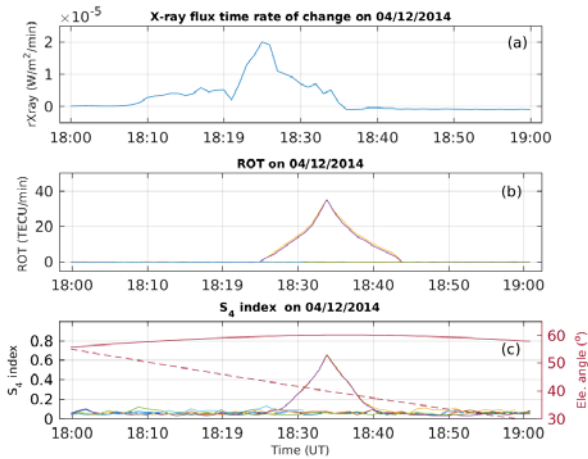


Fig. 4 Variations of rXray (a), ROT (b) and S_4 index (c) on December 4th 2014 from 18:00 to 19:00 UT.

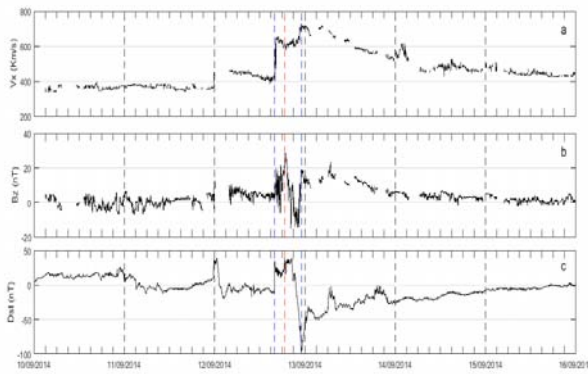


Fig. 5 Variations of the x component of the solar wind V_x (a), the z component of the interplanetary magnetic field (b) and the Dst index (c) from September 10th to 15th 2014.

analyzed on the basis of the magnetic parameters that are the x component of the solar wind speed, z component of the interplanetary magnetic field and Dst index recorded from 10 to 15 September 2014. Fig. 5 presents the variation of the magnetic parameters listed above. The x component of the solar wind V_x presents a regular variation with an average speed of 360 km/s until September 11th around midnight where it appears a small shock of 480 km/s.

During that period, B_z does not show any particular variation, it fluctuates around 0 nT (middle) as well as the Dst index until midnight September 11th where it is observed a peak of +40 nT (lowest panel). V_x decreases sharply from 480 km/s to 400 km/s followed by a shock with a speed above 640 km/s at 16:00 UT on September 12th. At the same time

it is observed an increasing of a northward B_z . The Dst index shows a sudden increasing at 16:00 UT on September 12th corresponding to SSC (storm sudden commencement).

There follows the compression phase of the storm until 19:30 UT. The northward B_z increases during the compression phase of the storm and reached a maximum value of +28 nT. The main phase of the storm is developed in the time ranging from 20:00 UT to 23:30 UT on September 12th. During that phase of the storm, the IMF B_z turns southward in the meantime and V_x increases at a high speed above 720 km/s. The main phase of the storm ended with a minimum value of the Dst index equal to -100 nT observed at 23:30 UT on September 12th. The recovery phase of the storm starts at 23:30 UT and lasted for several hours until September 15th. During that phase of the storm, it is observed a decreasing of the solar wind component V_x gradually from its maximum value to its average of value 400 km/s. There is an inversion of the IMF B_z component followed by a gradual decreasing. The effects observed on V_x , B_z and Dst index occurred approximately between forty six (46) and fifty eight (58) hours after the event of the X1.66 Class solar flare was observed on September 10th, 2014 at 17:55 UT. Fig. 6 presents the variation of the ionospheric VTEC observed (black curve) and that of the reference VTEC referred to us by $\langle vTEC_{quiet} \rangle$ (red curve) computed using the five (5) quietest days of the

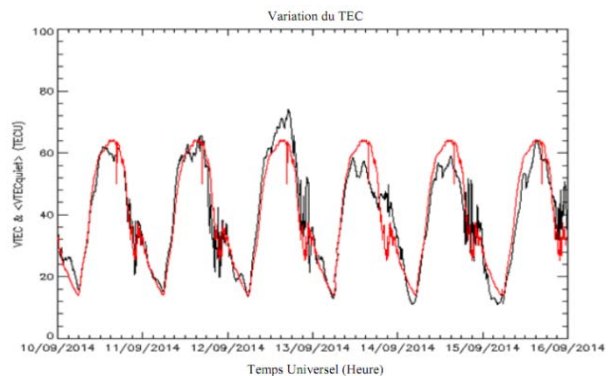


Fig. 6 Variations of the $VTEC_{observed}$ (black curve) and $\langle vTEC_{quiet} \rangle$ (red curve) from September 10th to 15th 2014.

representative month. The variation of the observed TEC is almost the same as that of the reference VTEC from September 10th to September 12th at 12:00. The VTEC_{observed} deviates from $\langle VTEC_{quiet} \rangle$ between 12:00 UT and 20:00 UT on September 12th. The observed VTEC increases 20% more than the reference VTEC value. From September 13th (06:00 UT) to September 15th, the observed VTEC value remains in general 10% lower than that of the $\langle VTEC_{quiet} \rangle$. The maximum value of VTEC during that time range oscillates around 58 TECU. This peculiarity of the VTEC appears to be related to the magnetic storm resulted from the solar flare that occurs on September 10th at 17:55 UT. The maximum value of the VTEC (76 TECU) is noted on September 12th around 18:00 UT corresponding to the beginning of the main phase of the storm. This delayed effect of the solar flare is observed almost 42-58 hours after the solar flare X1.66 class was observed at 17:55 UT on September 10th 2014.

3.3 Study of the Magnetic Storm 6-7 December 2014

Fig. 7 presents the variations of V_x , B_z and Dst index from 04 to 09 December 2014. It is noticed a variation of V_x at an average speed around 500 km/s until December 6th at 09:00 UT. Where it is observed a gradual increase of V_x to a peak value estimated to 760 km/s at 23:00 UT the same day. During that period of increase of V_x , it is noticed a positive variation of B_z with a maximum value of +20 nT reached at 18:00 UT. It is observed the increasing of the Dst index from +10 nT to a peak value of +40 nT reached at 15:00 UT on December 6th. It follows a decreasing of the Dst from +40 nT to a minimum value of -20 nT reached at 00:00 on December 7th. This time period can be attributed to the main phase of the storm. This phase of the variation of the Dst index is followed by the recovery phase that lasted until December 10th. As for B_z and Dst index, they practically show no major effects from 04 to 09 December 2014 except the time range of the

increasing of V_x . Fig. 8 describes the variation of observed VTEC compared to its reference value referred by $\langle VTEC_{quiet} \rangle$ from 04 to 09 December 2014. This figure indicates clearly that the VTEC_{observed} presents some particular characteristics between 12:00 UT on 06 December and 00:00 UT on December 7th, compared to the $\langle VTEC_{quiet} \rangle$. The reason lies in the fact that the different peaks values observed on the VTEC remain lower or equal to that of the reference one $\langle VTEC_{quiet} \rangle$. It is particularly during on December 6th between 12:00 UT and 24:00 UT, namely between forty-two (42) to fifty four (54) hours after the occurrence of the M6.16 Class solar flare occurred at 18:25 UT on December 4th that the VTEC observed shows two (2) well-marked peaks. The first peak equal

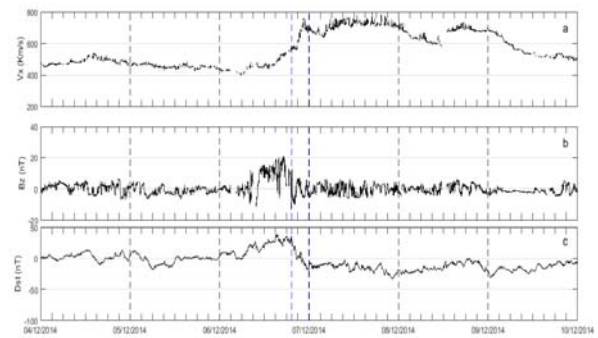


Fig. 7 Variations of the x component of the solar V_x (a), the z component of the interplanetary magnetic field (b) and the Dst index (c) from December 4th to 9th 2014.

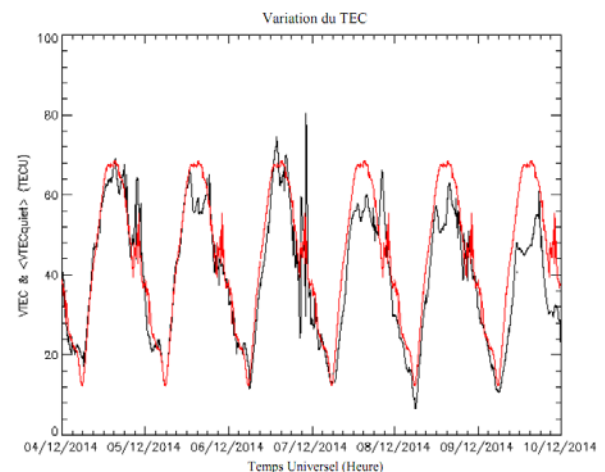


Fig. 8 Variation of the VTEC_{observed} (black curve) and $\langle VTEC_{quiet} \rangle$ (red curve) from December 4th to 9th 2014.

to 75 TECU (10.3% more than $\langle VTEC_{quiet} \rangle$ maximum) is noticed around 15:00 UT whereas the second peak, greater than the previous peak and equal to 81 TECU (20% more than $\langle VTEC_{quiet} \rangle$ maximum), is highlighted around 23:30 UT. From 07 to 09 December, the $VTEC_{observed}$ maximum values remain constantly below that of the $\langle VTEC_{quiet} \rangle$ until falling to 60 TECU (12% below $\langle VTEC_{quiet} \rangle$ maximum) on December 9th 2014.

4. Discussion and Conclusions

The investigation of the ionospheric response to M-Class and X-Class solar flares has revealed several interesting features. The present results are important because, it is the first time, attempt has been made to analyze the GPS data in order to study the effect of moderate and extreme solar flare on Abidjan Station in recent year 2014, after the solar maximum year 2013. This study shows that M-Class or X-Class solar flares exhibit simultaneous and/or delay effects on African equatorial ionospheric TEC confirm with the scintillation level with well-defined characteristics as demonstrated by the work of Davies [4]. The simultaneous effect of M and X class solar flare on the TEC is shown by a high rate of change of the TEC (e.g., $ROT > 35$ TECU/min) and a high S_4 index (e.g., $S_4 > 0.8$) between ten (10) and twelve (12) minutes after the occurrence of the peak of the solar X-ray flux rate of change (e.g., $rX_{ray} > 10^{-5}$ W/m²/min). The ROT value we obtained is higher than the 24 TECU/min observed by Kumar and Singh [13] during the weak solar flares of C and B Class in 2008, a year of low solar activity over Varanasi. The time delay remains slightly above 8.3 min after which Davies [4] observed various sudden ionospheric disturbances, including a sudden decrease in HF (high-frequency) signals or SWF (shortwave fadeout) signals in the D-layer as well as a sudden change in the frequency of the reflected HF signals or SFD (sudden frequency deviation) in the E-layer and a high increase in the electron density in the F-layer.

Moreover, for the same level of solar flares class, the maximum value observed in the ROT or the scintillation index S_4 generally decreases with that of the rate of change of solar flux associated. The maximum value of the scintillation index S_4 or TEC rate of change increase is related not only to the flare class but also to the time rate of change in flare radiations. These results are similar to those of Lui et al. [9] who determined good correlation coefficients between the TEC rate of change and the solar flare class on one hand and between the TEC rate of change and the time rate of change in flare radiations on the other hand. The study of the x component of the solar wind V_x , the z component of the interplanetary magnetic field B_z , the Dst index and the TEC during a time of six (6) days following the occurrence of the solar flare has highlighted the delay effect of the solar flare on the ionosphere. Indeed, delayed perturbations of the solar flare on the TEC over the station of Abidjan occur within 42 to 54 hours after an M-class solar flare and within 46 to 58 hours following an X-Class solar flare for the cases we have investigated. This time interval is within the limits time range of Pereira [14] and Davies [4] who observed propagating interplanetary disturbances such as magnetic storms and ionospheric storms. This delayed effect time coincides almost with that of Shimeis et al. [6] who found that the impact of the solar flare that has occurred on April 3rd, 2010 affected the Earth space environment on April 5th 2010 at 08:25 UT.

The delayed impact of the solar eruption on the ionosphere above the SCINDA station of Abidjan is associated with high increase of V_x up to 760 km/s, significant fluctuations of B_z marked by an increase at least 32 nT of amplitude, a remarkable magnetic storm with a main phase more or less abrupt (amplitude between 60 nT and 135 nT) as soon as a maximum TEC observed which sometimes reaches 20% above the maximum reference. It results a gradual reduction of the maximum values of the TEC observed to at least 10% below the maximum reference, forty-eight

(48) hours thereafter under conditions where the V_x and B_z observe lower values while the storm is near the end of its recovery phase.

This increase in the TEC is probably due to the increase in EUV radiation associated with the solar flare, consequently improved the ionization production and also the changes in the overall dynamic or electrodynamics of the low ionosphere due to the geomagnetic activity initiated after the advent of the solar flare [15].

This result is almost in agreement with that of Shimeis et al. [6] who observed that the shock that occurred on April 5th 2010 is associated with a strong V_x component of the solar wind ($V_x \sim 800$ km/s), a southern variation of the interplanetary magnetic field component ($B_z \sim 19$ nT) and an increase of the Dst index at the moment of the shock (Chapman Ferraro current at the front of the magnetosphere) followed by a decrease of this index illustrating the variations of the current flowing in the equatorial plane of the magnetosphere. Moreover, they noticed that during the days following the 06, 07 and 08 April 2010, the influence of the solar wind and the interplanetary magnetic field remained stable under values below their respective maximum before reaching to normal state more than forty-eight (48) hours after. They also observed that the TEC underwent a 25% increase at the time of the shock on April 5th 2010 and then decreased. The following days, they found a decrease in the TEC of about 25%. All these observations confirm the consistency of our hypotheses and analytical methods.

Acknowledgement

The authors are grateful to the Institute for Scientific Research at Boston College for making available the GNSS data of the Scintillation Decision and Aid (SCINDA) project used in this work. The authors also thank the International service of geomagnetism indices, the Goddard Space Flight Center OMNI web, the National Oceanic and

Atmospheric Administration (NOAA) and the Centre d'Information Géographique et du Numérique (CIGN) of the Bureau National d'Etudes Techniques et de Développement (BNETD) for hosting the SCINDA GPS receiver in Côte d'Ivoire.

References

- [1] Gopalswamy, N. 2009. "The Sun and Earth's Space Environment." In *Proceeding of the 2009 International Conference on Space Science and Communication, Negeri Sembilan, Malaysia*, 5-10.
- [2] Mahajan, K. K., Lodhi, N. K., and Singh, S. 2009. "Ionospheric Effects of Solar Flares at Mars." *Geophys. Res. Lett.* 36: L15207 05870980.
- [3] Mitra, A. P. 1974. "Ionospheric Effects of Solar Flares." New York: Springer.
- [4] Davies, K. 1990. *Ionospheric Radio*. London: Peter Peregrinus.
- [5] Basu, S., Basu, Su., Mackenzie, E., Bridgwood, C., Valladares, C. E., Groves, K. M., and Carrano, C. 2010. "Specification of the Occurrence of Equatorial Ionospheric Scintillations during the Main Phase of Large Magnetic Storms within Solar Cycle 23." *Radio Science* 45: RS5009, doi:10.1029/2009RS004343.
- [6] Shimeis, A., Fathy, I., Amory-Mazaudier, C., Fleury, R., Mahrous, A. M., Yumoto, K., and Groves, K. M. 2012. "Signature of the Coronal Hole near the North Crest Equatorial Anomaly over Egypt during the Strong Geomagnetic Storm 5 April 2010." *J. Geophys. Res.* 117: A07309, doi:10.1029/2012JA017753.
- [7] Gwal, A. K., Bhawre, P., Mansoori, A. A., and Khan, P. A. 2013. "Study of GPS Derived Total Electron Content and Scintillation Index Variations over Indian Arctic and Antarctic Stations." *Journal of Scientific Research* 5 (2): 255-64.
- [8] Sharma, S., Chandra, H., Vats, H. O., Pandya, N. Y., and Jain, R. 2010. "Ionospheric Modulations due to Solar Flares over Ahmedabad." *Indian J. Radio and Space Phys.* 39: 296-301.
- [9] Lui, J. L., Lin, C. H., Chen, Y. I., Lin, Y. C., Fang, T. W., Chen, C. H., and Chen, Y. C. 2006. "Solar Flare Signatures of the Ionospheric GPS Total Electron Content." *J. Geophys. Res.* 111: A05308, doi:10.1029/2005JA011306.
- [10] Basu, S., Mackenzie, E., and Basu, Su. 1988. "Ionospheric Constraints on VHF/UHF Communication Links during Solar Maximum and Minimum Periods." *Radio sci.* 23: 363-78.
- [11] Carrano, C., and Groves, K. 2006. "The GPS Segment of the AFRL-SCINDA Global Network and the Challenges

- of Real-Time TEC Estimation in the Equatorial Ionosphere.” In *Proceeding of the Institute of Navigation NTM*, Monterey, CA.
- [12] Otsuka, Y., Shiokawa, K., and Ogawa, T. 2006. “Equatorial Ionospheric Scintillations and Zonal Irregularity Drifts Observed with Closely-Spaced GPS Receivers in Indonesia.” *Journal of the Meteorological Society of Japan* 84A: 343-51.
- [13] Kumar, S., and Singh, A. K. 2012. “Effect of Solar Flares on Ionospheric TEC at Varanasi, near EIA Crest, during Solar Minimum Period.” *Indian J. Radio and Space Phys.* 41: 141-7.
- [14] Pereira, F. 2004. “Analyse spatio-temporelle du champ géomagnétique et des processus d'accélération solaires observées en émission radio.” Ph.D. Thesis, Univ. Orléans.
- [15] Tsurutani, B. T., Judge, D. L., Guarnieri, F. L., Gangopadhyay, P., Jones, A. R., Nuttall, J., Zambon, G. A., Didkovsky, L., Mannucci, A. J., Iijima, B., Meier, R. R., Immel, T. J., Woods, T. N., Prasad, S., Floyd, L., Huba, J., Solomon, S. C., Straus, P., and Viereck, R. 2005. “The October 28, 2003 Extreme EUV Solar Flare and Resultant Extreme Ionospheric Effects: Comparison to Other Halloween Events and the Bastille Day Event.” *Geophys. Res. Lett.* 32: L03S09.